

Comparative catalytic activity of supported ZnBr₂-containing ionic liquid catalysts for preparation of glycerol carbonate by glycerolysis of urea

Dong-Woo Kim, Min-Ji Kim, Kuruppathparambil Roshith, Moon-Il Kim, Joo-Young Kwak, and Dae-Won Park[†]

School of Chemical and Biomolecular Engineering, Pusan National University, Busan 609-735, Korea
(Received 5 October 2013 • accepted 28 December 2013)

Abstract—The synthesis of glycerol carbonate by glycerolysis of urea was investigated under mild conditions, using immobilized metal-containing ionic liquid catalysts. Three different catalysts were prepared, with the following supports: (1) polystyrene (PS), (2) commercial silica (CS), and (3) chitosan (CH). The glycerolysis of urea was considered to include two main reactions: carbamylation of glycerol and carbonylation of glycerol carbamate. The approximate rate constant for PS-(Im)₂ZnBr₂ was higher than those of CH-(Im)₂ZnBr₂ and CS-(Im)₂ZnBr₂ probably due to its well-balanced acid-base properties. The activation energies for PS-, CH-, and CS-(Im)₂ZnBr₂ were 142.9, 163.0, and 166.7 kJ mol⁻¹, respectively. PS-(Im)₂ZnBr₂ exhibited better reuse properties than CH-(Im)₂ZnBr₂ and CS-(Im)₂ZnBr₂ catalysts.

Keywords: Glycerol Carbonate, Glycerol, Urea, Supported Catalyst, Ionic Liquid

INTRODUCTION

Increasing attention has been focused on the use of glycerol, a by-product with the amount at one-tenth of biodiesel production, to produce value-added chemicals [1]. Among the chemicals derived from glycerol, glycerol carbonate (GC) is a highly value-added product with many potential applications [2-6]. It is attractive for its low toxicity, good biodegradability, and high boiling point. It has been investigated as a novel component of gas separation membranes, polyurethane foams [7], and surfactants [8], a nonvolatile reactive solvent for several types of materials, and a component of coatings, paints, and detergents.

The main methods for the preparation of GC are based on the reaction of glycerol with (a) phosgene and a dialkyl carbonate or an alkylene carbonate, (b) carbon monoxide and oxygen or carbon dioxide, or (c) urea. GC has traditionally been prepared by the reaction of glycerol with phosgene; however, because of the high toxicity and corrosive nature of phosgene, alternative methods for the preparation of GC, such as the transesterification of dialkyl or alkylene carbonates with glycerol, have been explored [7]. A method based on the reaction of glycerol with carbon monoxide and oxygen under high pressure in the presence of a catalyst is also known [8]. However, more cost-effective and simpler methods involving the use of very safe materials are needed. Aresta et al. [9] investigated the direct carboxylation of glycerol with carbon dioxide (5 MPa) at 177 °C, using transition-metal alkoxides. However, the yield of GC obtained was very low.

An alternative method for the synthesis of GC is the glycerolysis of urea, a reaction recently described in the literature [10-12]. The main advantage of this method is that the reactants, glycerol and urea, are inexpensive and easily available raw materials, which are

neither explosive nor poisonous. In addition, the NH₃ that is usually generated when GC is synthesized from urea and glycerol can be easily converted back to urea by reacting with carbon dioxide.

Much effort has been devoted to finding effective catalysts for the glycerolysis of urea. Homogeneous catalysis using inorganic salts such as ZnSO₄ [13], MgSO₄ [14], and ZnO [15] has been described, and, recently, certain heterogeneous systems based on these oxides have also been reported [16,17].

Polymer-supported catalysts are extensively used in both industry and academia because of the advantages they offer compared to homogeneous catalysts [18-20], including easy handling of odorous and toxic substances, and the possibility of achieving site isolation, which increases the catalytic activity, selectivity, and shelf life [19, 21]. Chitosan (CH)-like biopolymers, which have large numbers of hydroxyl groups, are efficient and natural support materials. CH, the second most abundant polysaccharide found on earth next to cellulose, is an attractive biopolymer for catalytic applications because of its low cost, biocompatibility, biodegradability, and nontoxicity [22]. Chitosan is a much more environmentally friendly support than synthetic polymers. Since the discovery of ordered mesoporous silica [23], continuous efforts have been made to improve its stability and catalytic performance. Recently, the incorporation of 3-chloropropylmethyl substituents on commercial and amorphous silica was reported [24,25].

In our previous work [26], we studied the synthesis of GC from urea and glycerol using metal containing ionic liquid (MIL) as catalyst. In the present study, the same reaction was performed using MILs immobilized on various supports. We prepared three differently supported MIL catalysts to compare their activities: polystyrene (PS), commercial silica (CS), and chitosan (CH, biopolymer). A comparative kinetic study of reactions with the immobilized MIL catalysts was carried out under mild conditions without any solvent. Moreover, to investigate the catalyst stability, recycling tests were performed, under the same conditions, on the three different immobilized MIL catalysts.

[†]To whom correspondence should be addressed.

E-mail: dwpark@pusan.ac.kr

Copyright by The Korean Institute of Chemical Engineers.

EXPERIMENTAL

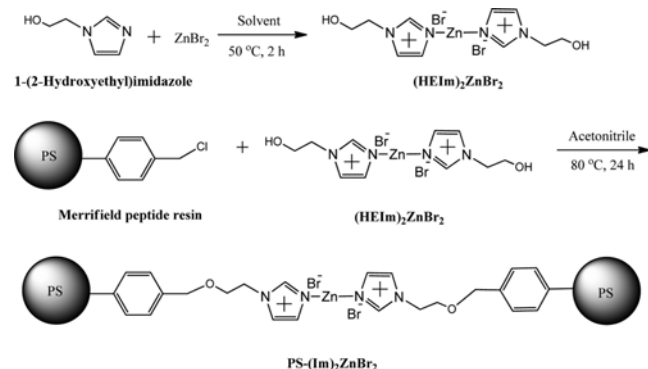
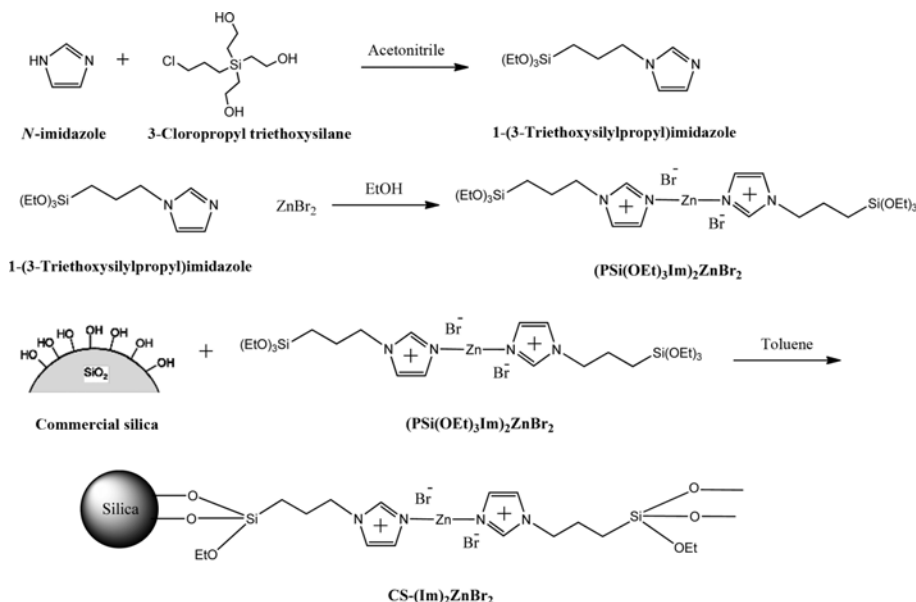
1. Materials

High-purity (>99%) *N*-imidazole, 1-(2-hydroxyethyl)imidazole, 3-chloropropyltriethoxysilane (CIPTES), 1,2-dibromoethane, zinc bromide, Merrifield's peptide resin (MPR, 1% divinylbenzene, 4.0 mmol Cl/g), commercial silica, and chitosan were purchased from Sigma-Aldrich. Glycerol (>99%), urea (>99%), GC (>99%), and methanol (>99%) were obtained from Sigma-Aldrich. All materials were used without further purification.

2. Synthesis of Supported Metal Containing Ionic Liquid (S-MIL) Catalysts

2-1. PS-(Im)₂ZnBr₂

The synthesis of a polymer-supported MIL based on Zn-imidazolium bromide, PS-(Im)₂ZnBr₂, was performed in two steps, as shown in Scheme 1. First, bis[1-(2-hydroxyethyl)imidazolium]zinc bromide, (HEIm)₂ZnBr₂, was prepared by metal insertion as follows. An ethanol solution (100 mL) containing 1-(2-hydroxyethyl)imidazole (40 mmol) was added to an ethanol solution (100 mL) con-

Scheme 1. Preparation of PS-(Im)₂ZnBr₂.Scheme 2. Preparation of CS-(Im)₂ZnBr₂.

taining zinc bromide (20 mmol). This mixture was stirred for 2 h at 50 °C and then filtered. A crystalline solid was obtained after drying at 100 °C for 24 h under vacuum.

Then (HEIm)₂ZnBr₂ was introduced onto MPR by alkoxylation, as described in our previous reports [27,28]; a mixture of MPR (5 g, 20 mmol Cl/g), (HEIm)₂ZnBr₂ (10 mmol), and acetonitrile (100 mL) was heated at 80 °C for 48 h in a 250 mL round-bottomed flask with a condenser. After cooling to room temperature, a brown solid was collected by filtration and washed several times with ethanol. The solid was dried at 80 °C for 24 h under vacuum.

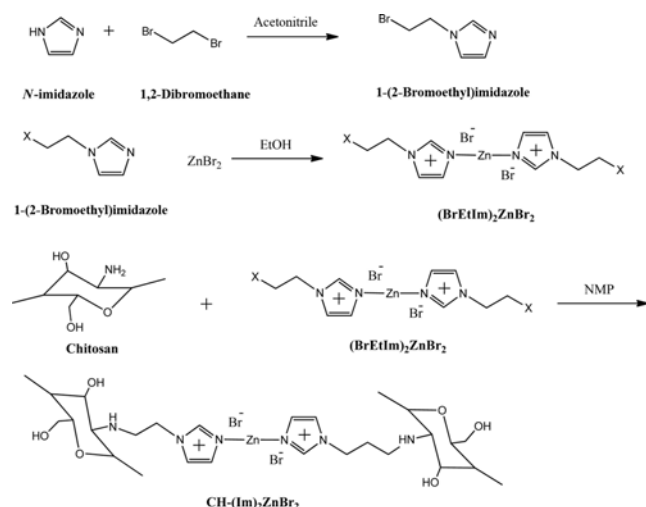
2-2. CS-(Im)₂ZnBr₂

The immobilization on commercial silica of an MIL based on Zn-imidazolium bromide, CS-(Im)₂ZnBr₂, was also performed in two steps. Bis[1-(3-triethoxysilylpropyl)imidazolium] zinc bromide, [PSi(OEt)₃Im]₂ZnBr₂, was prepared using the procedure shown in Scheme 2. In a typical procedure, imidazole (40 mmol) was added to a flask containing 50 mL of acetonitrile; CIPTES (7.3 mL) was poured into the solution and the mixture was refluxed at 80 °C for 12 h under an argon atmosphere. 1-(3-Triethoxysilylpropyl)imidazole was obtained after removal of the solvent under vacuum. Metal insertion into 1-(3-triethoxysilylpropyl)imidazole was then carried out using the method described above.

Grafting experiments were performed using the following procedure [24,25]. Prior to immobilization, commercial silica was purified using hot Piranha solution (H₂O₂ and H₂SO₄), followed by rinsing with water and drying under a stream of nitrogen. The pretreated CS (4 g) and [PSi(OEt)₃Im]₂ZnBr₂ (20 mmol) were codispersed in anhydrous toluene in a flask. The mixture was refluxed at 100 °C for 48 h under a nitrogen atmosphere. The resultant product was filtered and washed with dichloromethane and ethanol to remove excess MIL. The residual solvent was evaporated in a vacuum oven, giving CS-(Im)₂ZnBr₂.

2-3. CH-(Im)₂ZnBr₂

The CH-supported MIL based on a Zn-imidazolium bromide catalyst, CH-(Im)₂ZnBr₂, was synthesized in two steps (Scheme 3).



Scheme 3. Preparation of $\text{CH}-(\text{Im})_2\text{ZnBr}_2$.

For the preparation of bis(bromoethylimidazolium) zinc bromide, $(\text{BrEtIm})_2\text{ZnBr}_2$, dibromoethane (40 mmol) was dissolved in 50 mL acetonitrile, and then added slowly to *N*-imidazole (40 mmol) in acetonitrile under nitrogen atmosphere in a 100 mL two-neck round bottomed flask. The mixture was refluxed at 80 °C for 12 h. $(\text{BrEtIm})_2\text{ZnBr}_2$ was generated by metal insertion.

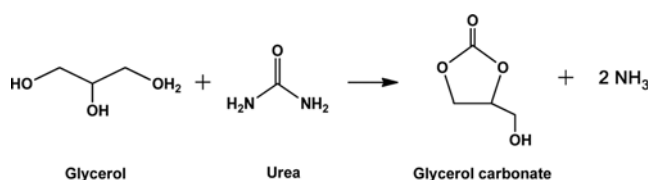
In the covalent immobilization of $(\text{BrEtIm})_2\text{ZnBr}_2$ on chitosan [29], chitosan (2 g) was added to 40 mL of 1-methyl-2-pyrrolidinone (NMP), and the mixture stirred at 50 °C for 12 h in a two-necked flask. $(\text{BrEtIm})_2\text{ZnBr}_2$ (10 mmol in 10 mL of NMP) was added and the mixture stirred at 80 °C for 24 h. When the reaction was complete, the solid product was washed four to five times with dry ethanol. The sample was dried under vacuum at 80 °C for 24 h, giving $\text{CH}-(\text{Im})_2\text{ZnBr}_2$.

3. Characterization of S-MIL Catalysts

Elemental analysis (EA) was performed with a Vario EL III instrument. Samples (2 mg) were subjected to a temperature of 1,100 °C; sulfanilic acid was used as a standard. Fourier transform infrared (FT-IR) spectra were obtained with an AVATAR 370 Thermo Nicolet spectrometer at a resolution of 4 cm^{-1} . X-ray photoelectron spectroscopy (XPS) of the catalysts was conducted by using a Theta Probe AR-XPS system with monochromated Al $K\alpha$ radiation ($h\nu = 1,486.6$ eV). ^{29}Si solid-state nuclear magnetic resonance (NMR) spectroscopy was carried out at a frequency of 79.5 using an INOVA-400 WB magic-angle spinning (MAS) probe. ^{29}Si MAS-NMR spectra were obtained at room temperature using the following conditions: MAS at 5 kHz; $\pi/2$ pulse, 6.5 μs , and a repetition delay of 60 s; 3928 scans were performed, referenced to tetramethylsilane. Thermogravimetric analysis (TGA) was performed using an AutoTGA 2950 apparatus under a nitrogen flow of 100 mL min^{-1} , at a heating rate of 10 °C min^{-1} from room temperature to 500 °C.

4. Synthesis of GC from Glycerol and Urea

GC was synthesized from glycerol and urea (Scheme 4) in a 50 mL glass reactor equipped with a magnetic stirrer and condenser. In a typical reaction, the reactor was charged with the catalyst, glycerol, and urea. When the desired temperature was reached, the reaction was initiated by stirring under vacuum to remove the NH_3 formed as a by-product. The products and reactants were analyzed by gas



Scheme 4. Synthesis of glycerol carbonate from urea and glycerol.

chromatograph (HP 6890N) equipped with a flame ionization detector (FID) and a capillary column [HP-INNOWAX, poly(ethylene glycol)]. Tetraethylene glycol (TEG) was used as an internal standard. The conversion and selectivity were calculated based on the assumption that glycerol was a limited reactant.

RESULTS AND DISCUSSION

1. Characterization of Catalysts

1-1. $\text{PS}-(\text{Im})_2\text{ZnBr}_2$

To confirm the immobilization of the MIL based on Zn-imidazolium bromide on PS, FT-IR spectroscopy was performed; the spectra are shown in Fig. 1. In the FT-IR spectrum of $\text{PS}-(\text{Im})_2\text{ZnBr}_2$, the characteristic peak corresponding to the stretching frequency of CH_2Cl (1,265 cm^{-1}), which was present in the PS spectrum, disappeared, suggesting complete modification of MPR [30-32]; four new peaks that appeared at 1,610, 1,560, 1,145, and 1,070 cm^{-1} were associated with stretching frequencies of the imidazolium ring [32].

XPS analysis of $\text{PS}-(\text{Im})_2\text{ZnBr}_2$ confirmed the structure of the catalyst. The N 1s spectrum of $\text{PS}-(\text{Im})_2\text{ZnBr}_2$ is shown in Fig. 2. The $\text{PS}-(\text{Im})_2\text{ZnBr}_2$ catalyst contained a peak near 401.7 eV from nitrogen species originating from the positively charged nitrogen of imidazolium [29,33-36]. As can be seen from Fig. 3, the Br 3d spectrum of $\text{PS}-(\text{Im})_2\text{ZnBr}_2$ had a peak at 68.2 eV, which was assigned to negatively charged bromide ions [37]. These results are a

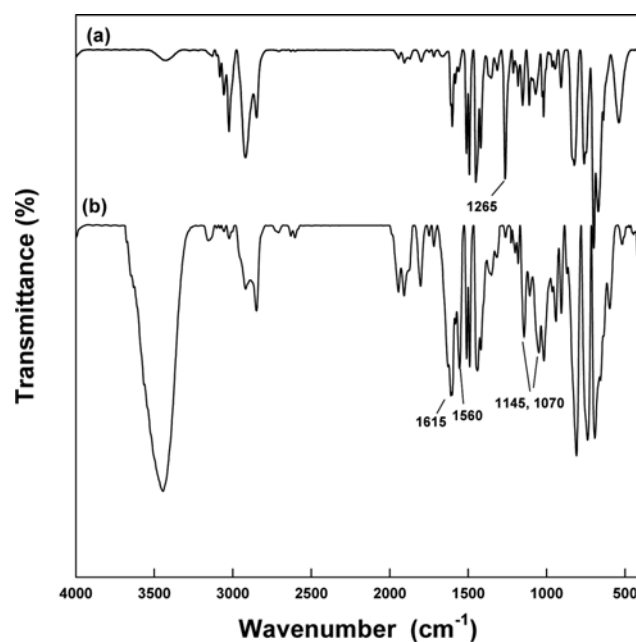
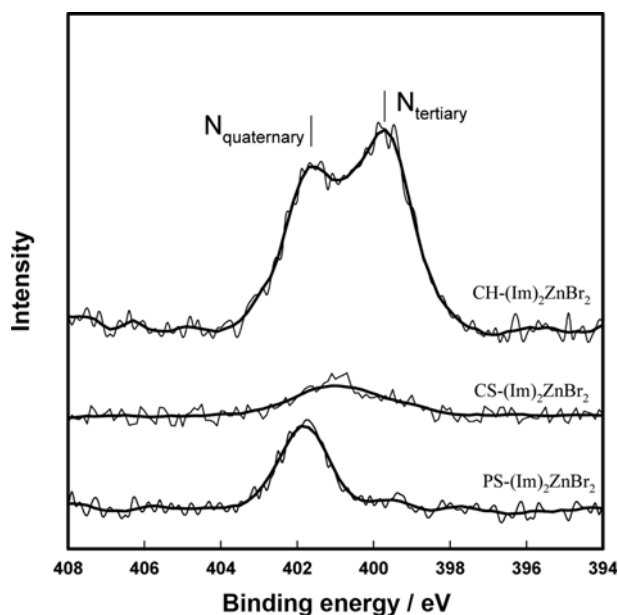
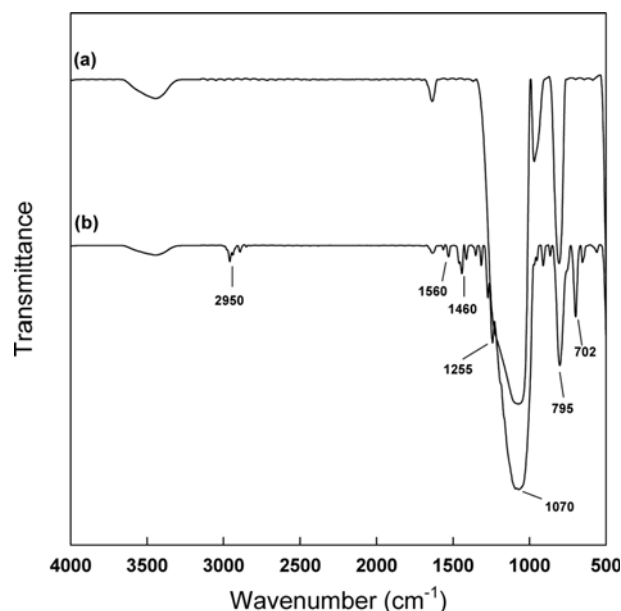
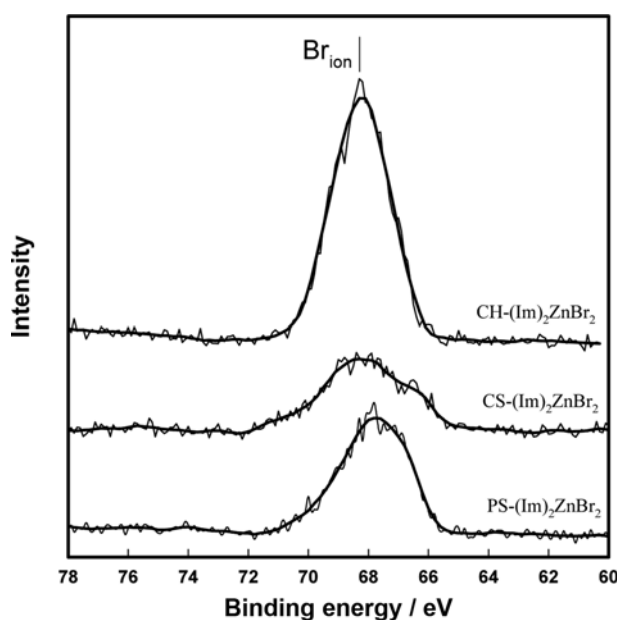


Fig. 1. FT-IR spectra of (a) polystyrene, (b) $\text{PS}-(\text{Im})_2\text{ZnBr}_2$.

Fig. 2. XPS N 1s spectra of S-(Im)₂ZnBr₂ catalysts.Fig. 4. FT-IR spectra of (a) commercial silica, (b) CS-(Im)₂ZnBr₂.Fig. 3. XPS Br 3d spectra of S-(Im)₂ZnBr₂ catalysts.

clear indication of covalent immobilization of MIL as active sites on the PS support, as shown in Scheme 1.

Elemental analysis results for the materials are shown in Table 1; the MIL loading on PS-(Im)₂ZnBr₂, based on nitrogen, was calculated to be 0.66 mmol per gram of PS.

1-2. CS-(Im)₂ZnBr₂

Qualitative identification of the MIL based on Zn-imidazolium bromide functional groups on CS was also performed using FT-IR spectroscopy (Fig. 4). Typical Si-O-Si bands at 1,225, 1,070, and 795 cm⁻¹, associated with the condensed silica network, were present in the FT-IR spectra of both CS and CS-(Im)₂ZnBr₂, [24,25]. However, CS-(Im)₂ZnBr₂ exhibited the characteristic bands of aromatic C-H stretching at 2,950 cm⁻¹, ring stretching of the imidazolium molecule at 1,560 and 1,460 cm⁻¹, and C-Si stretching at 702 cm⁻¹; the C-Si stretching band was not present in the CS spectrum [25, 32].

To investigate the efficiency of the grafting reaction, solid-state ²⁹Si MAS-NMR analysis of CS-(Im)₂ZnBr₂ was carried out. As shown in Fig. 5, two peaks, centered at -102 and -111 ppm, corresponding to Q₃ [Si(OSi)₃(OH)] and Q₄ [Si(OSi)₄] silicon atoms, respectively, were observed. The peaks situated at -78.8, -67.4, and -59.8 ppm were assigned to T₃ [Si(OSi)₃R], T₂ [Si(OSi)₂R(OH)], and T₁ [Si(OSi)₃R(OH)₂] organosiloxanes, indicating incorporation of the MIL functional moiety into the CS [25,28,38].

The XPS N 1s and Br 3d spectra of CS-(Im)₂ZnBr₂, shown in Figs. 2 and 3, respectively, had an N 1s peak at 401.4 eV from posi-

Table 1. Elemental analysis of S-(Im)₂ZnBr₂ catalysts

Catalyst	CHNO from elemental analysis				Amount of MIL ^a (mmol/g)
	C (wt%)	N (wt%)	O (wt%)	H (wt%)	
PS-(Im) ₂ ZnBr ₂	63.88	3.68	2.41	-	0.66
CS-(Im) ₂ ZnBr ₂	41.36	7.78	38.15	-	1.4
CH-(Im) ₂ ZnBr ₂	23.47	30.54	3.48	5.52	1.12
Chitosan	40.3	42.88	7.2	6.92	-

^aAmount of MIL immobilized onto support

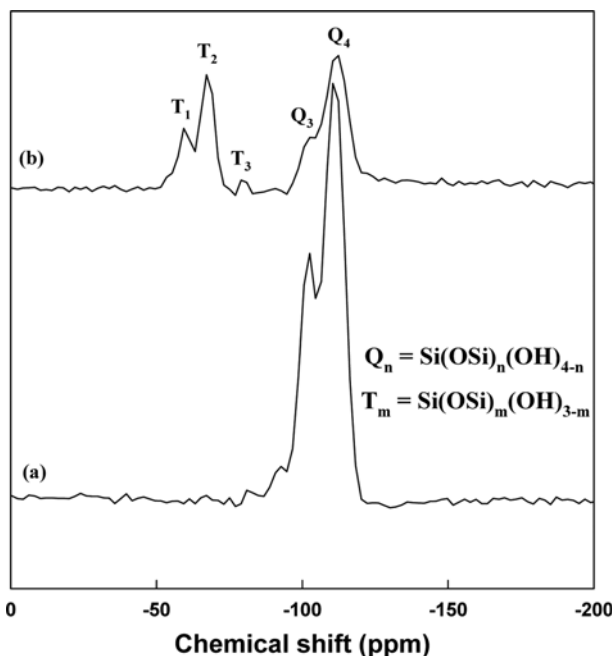


Fig. 5. ^{29}Si solid state NMR spectra of (a) commercial silica, (b) CS-(Im) $_2$ ZnBr $_2$.

tively charged nitrogen and a Br 3d peak at 68.1 eV from negatively charged bromide ions. The amount of grafted MIL was determined based on elemental analysis. The amount of grafted MIL, based on nitrogen, was calculated to be 1.4 mmol per gram of CS (Table 1). These results indicate that the MIL was successfully grafted onto the CS surface, as shown in Scheme 2.

1-3. CH-(Im) $_2$ ZnBr $_2$

The successful covalent immobilization of the MIL based on Zn-imidazolium bromide on the CH surface was confirmed using FT-IR and XPS analysis. As shown in Fig. 6, a broad peak at 3,500 cm^{-1} , assigned to O-H and N-H stretching vibrations [29,33], and a

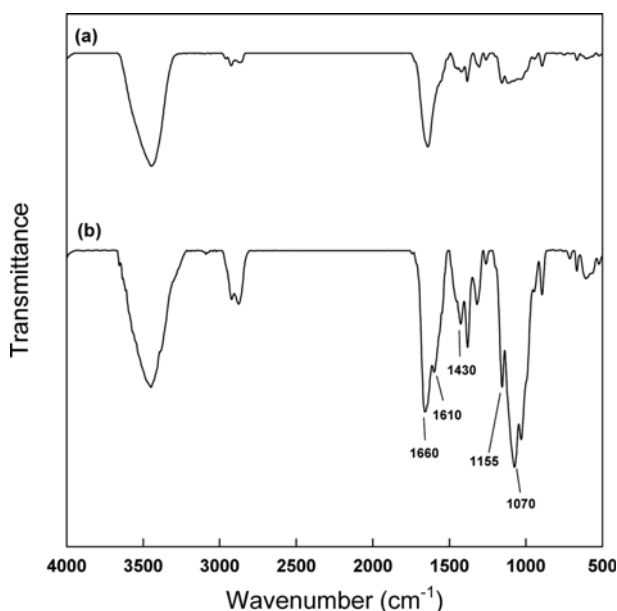


Fig. 6. FT-IR spectra of (a) chitosan, (b) CH-(Im) $_2$ ZnBr $_2$.

Table 2. Reactivity of S-(Im) $_2$ ZnBr $_2$ catalysts on the synthesis of GC by glycerolysis of urea

Catalyst	X_G (%)	S_{GC} (%)	Y_{GC} (%)	TON a
PS-(Im) $_2$ ZnBr $_2$	65.8	72.3	47.6	156.8
CS-(Im) $_2$ ZnBr $_2$	55.3	58.8	32.5	58.9
CH-(Im) $_2$ ZnBr $_2$	57.6	61.0	35.2	68.3

Reaction conditions: Urea=50 mmol, Glycerol=50 mmol, Cat.=5 wt% of glycerol, Temp.=140 $^{\circ}\text{C}$, Degree of vacuum=14.7 kPa, Reaction time=6 h

a TON=(mole of GC)/(mole of MIL)

peak at 1,660 cm^{-1} , corresponding to C-O stretching, were observed in the spectra of both CH and CH-(Im) $_2$ ZnBr $_2$. However, four peaks at 1,610, 1,430, 1,155, and 1,070 cm^{-1} , associated with stretching frequencies of the imidazolium ring, were only present in the CH-(Im) $_2$ ZnBr $_2$ spectrum.

The XPS N 1s spectrum of CH-(Im) $_2$ ZnBr $_2$ contained peaks at 398.8 and 401.5 eV (Fig. 2), arising from the amine groups of CH and imidazolium N $^+$, respectively [30,32]. The XPS Br 3d peak at 68.5 eV (Fig. 3) was assigned to negatively charged bromide ions. These results confirm that the structure of the CH-(Im) $_2$ ZnBr $_2$ catalyst is as shown in Scheme 3. The elemental analysis results for CH and CH-(Im) $_2$ ZnBr $_2$ are shown in Table 1. The Zn-IL loading for CH-(Im) $_2$ ZnBr $_2$ was calculated, based on Zn-Br $_2$, to be 1.12 mmol per gram of CH.

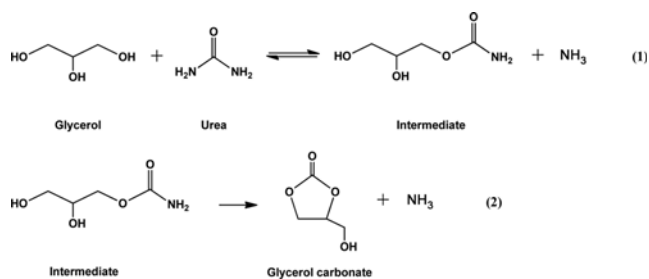
2. Comparative Activities of Different S-MIL Catalysts

To investigate the effects of different S-MIL catalysts on the glycerolysis of urea, PS-(Im) $_2$ ZnBr $_2$, CS-(Im) $_2$ ZnBr $_2$, and CH-(Im) $_2$ ZnBr $_2$ were examined under a vacuum pressure of 14.7 kPa for a reaction time of 6 h at 140 $^{\circ}\text{C}$. The data in Table 2 show that the glycerol conversions and turnover number (TON) of GC increased in the order CS-(Im) $_2$ ZnBr $_2$ <CH-(Im) $_2$ ZnBr $_2$ <PS-(Im) $_2$ ZnBr $_2$. We conclude that the CH- and CS-supported MILs have lower activities because of the more hydrophilic nature of the supports. It was clear from our previous study [26] that the hydrophilic character of the catalyst assists the adsorption of hydrophilic glycerol on the catalyst. However, too many hydroxyl groups on the surfaces of CS and CH may inhibit interactions between the active centers on the Zn-imidazolium bromide of the S-MIL and glycerol. In contrast, PS, which is hydrophobic, exposes the active centers to the glycerol substrate much more efficiently.

The activation energies of the S-MIL catalysts for glycerolysis of urea were calculated, to confirm the results of the comparison of the catalytic activities. The glycerolysis of urea to GC can be divided into two steps, as shown in Scheme 5: First, an intermediate is synthesized from urea and glycerol; then the intermediate is converted to GC [15,16]. For the synthesis of GC from urea and glycerol, the following elementary reaction steps are proposed, where G is glycerol, U is urea, I is the intermediate, A is NH $_3$, and GC is glycerol carbonate.



k_1 , k'_1 and k_2 are the reaction rate constants. Assuming that the first



Scheme 5. Proposed reaction steps for the glycerolysis of urea to produce glycerol carbonate.

step is at equilibrium and the next step is the rate-determining step, the rates of reaction of each step can be written as

$$r_1 = k_1 C_G C_U - k_1' C_I C_A \quad (3)$$

$$r_2 = k_2 C_I = \frac{1}{W} \frac{dC_{GC}}{dt} \quad (4)$$

W is the amount of catalyst and t is reaction time.

The concentration of each material can be described in terms of glycerol conversion (X_G) as follows:

$$C_G = C_{G_0}(1 - X_G) \quad (5)$$

$$C_U = C_{U_0}(1 - X_G) \quad (6)$$

$$C_{GC} = C_{G_0} X_G \quad (7)$$

$$C_A = 2C_{G_0} X_G \quad (8)$$

$$C_I = \frac{K_1 C_U (1 - X_G)^2}{2 X_G} \quad (9)$$

By applying Eqs. (5)-(9), Eq. (4) can be rewritten as

$$r_2 = \frac{C_{G_0} dX_G}{W dt} = k_2 \left[\frac{K_1 C_{U_0} (1 - X_G)^2}{2 X_G} \right] \quad (10)$$

$$K_1 = [C_{GC} C_A] / [C_G C_U] = k_1 / k_1'$$

Rearranging Eq. (10) gives

$$\frac{dX_G}{dt} = \frac{k_{app} W R_0 (1 - X_G)^2}{2 X_G} \quad (\text{where } k_{app} = k_2 K_1, R_0 = C_{U_0} / C_{G_0}) \quad (11)$$

Integration of Eq. (11) from $t=0$ to t gives

$$\frac{2}{W R_0} \left[\ln(1 - X_G) + \frac{1}{(1 - X_G)} - 1 \right] = k_{app} t \quad (12)$$

The slope of the linear plot of the left-hand side of Eq. (12), $f(X_G)$, versus time, can be used to estimate the approximate reaction rate constant k_{app} . The glycerolysis of urea was carried out using 5 wt% of catalyst based on glycerol, 50 mmol of glycerol, and 50 mmol of urea at 120-140 °C for 1-4 h.

The variations in glycerol conversion during the reactions with different S-MIL catalysts at different temperatures are shown in Fig. 7. Fig. 8 shows plots of $f(X_G)$ versus time for different S-MIL catalysts; the linear plot data fit the simulated kinetic equation well. The reaction rate constants of different S-MIL catalysts are listed in Table 3. It is obvious that the reaction temperature has a strong effect on the reaction rate constant. The order of the approximate reaction rate constants for the immobilized catalysts was PS-(Im)₂ZnBr₂ >

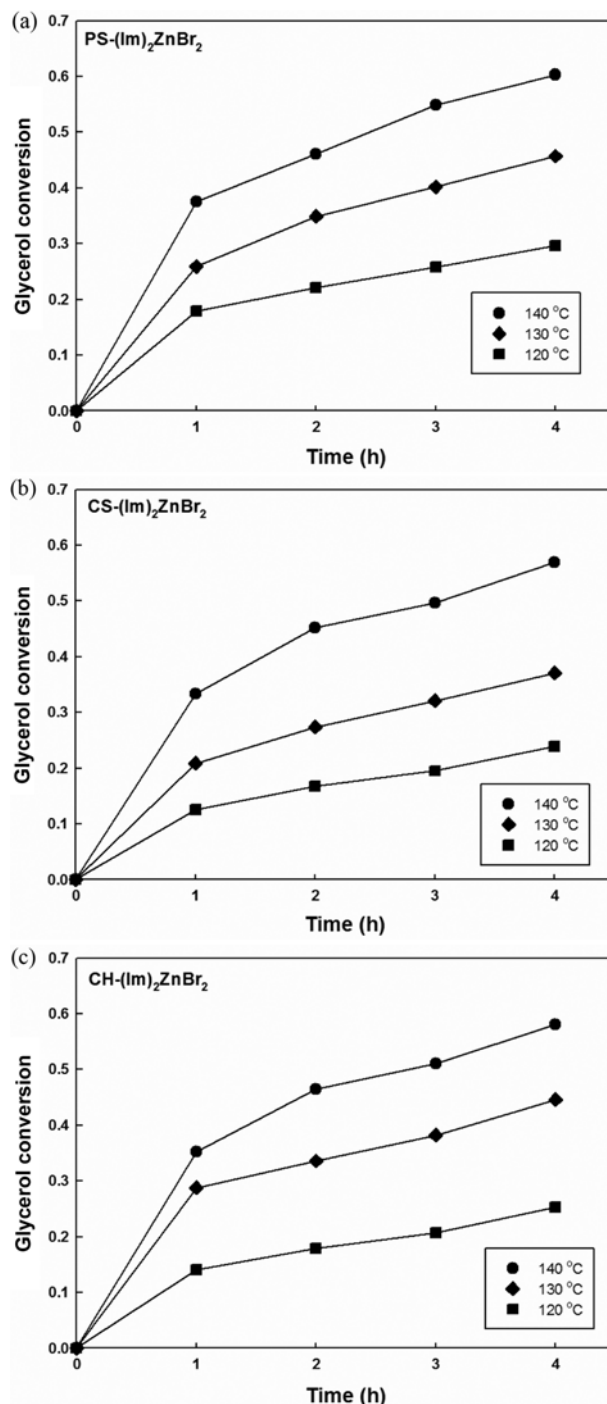


Fig. 7. Variation of glycerol conversion with time at different temperatures: (a) PS-(Im)₂ZnBr₂, (b) CS-(Im)₂ZnBr₂, (c) CH-(Im)₂ZnBr₂.

CH-(Im)₂ZnBr₂ > CS-(Im)₂ZnBr₂. PS-(Im)₂ZnBr₂ showed the highest activity probably because of its well-balanced acid-base properties [39]. Lewis acid sites activate the carbonyl group of urea and Lewis base sites activate the hydroxyl group of glycerol.

The relationship between the reaction rate constant k_{app} and the absolute temperature obeys the Arrhenius equation:

$$k_{app} = A \exp(E_{app}/RT) \quad (13)$$

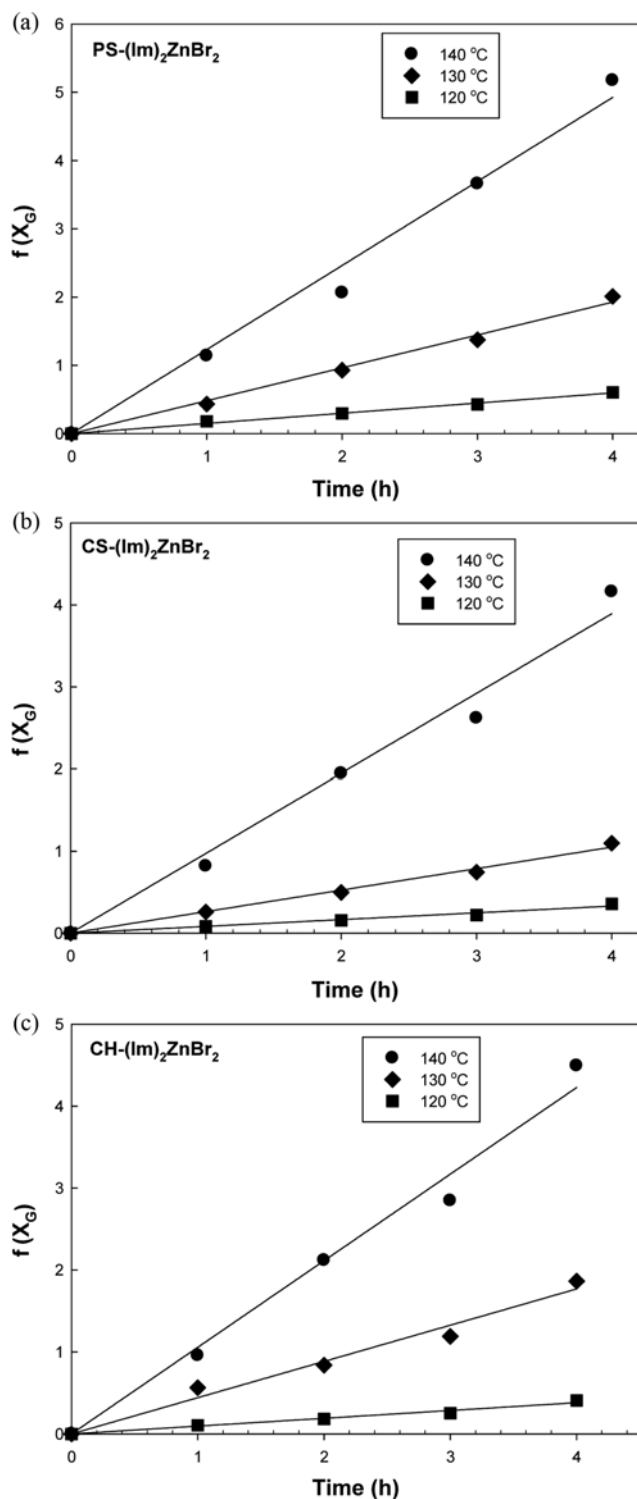


Fig. 8. Linear plot of $f(X_G)$ versus time at different temperatures: (a) PS-(Im)₂ZnBr₂, (b) CS-(Im)₂ZnBr₂, (c) CH-(Im)₂ZnBr₂.

where E_{app} is the approximate activation energy, A is a constant known as the pre-exponential factor, and T is the Kelvin temperature. The logarithmic form of Eq. (13) is

$$\ln k_{app} = -\frac{E_{app}}{RT} + \ln A \quad (14)$$

Table 3. Approximate reaction rate constants and activation energies

Temperature (°C)	Rate constant, k_{app} (molh ⁻¹ g ⁻¹)		
	PS-(Im) ₂ ZnBr ₂	CS-(Im) ₂ ZnBr ₂	CH-(Im) ₂ ZnBr ₂
120	0.1491±0.0034	0.0826±0.0035	0.0954±0.0041
130	0.4816±0.0113	0.2626±0.0064	0.4424±0.0193
140	1.2315±0.0439	0.9733±0.0395	1.0571±0.0393
E_{app} (kJ/mol)	142.9±7.1	166.7±8.4	163.0±6.9

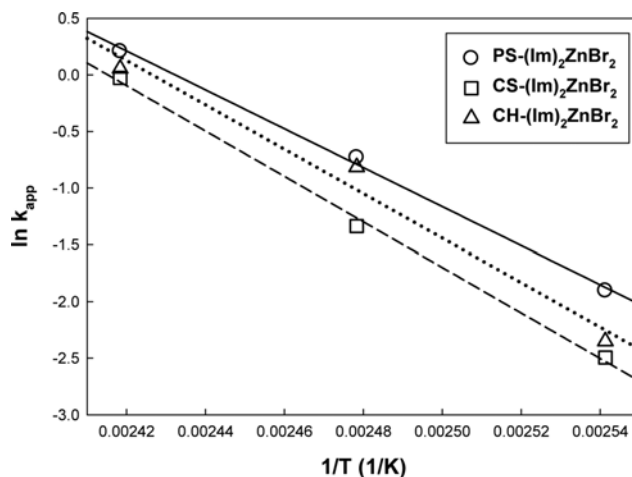


Fig. 9. Arrhenius plots of S-(Im)₂ZnBr₂.

Table 4. Recycle test of S-(Im)₂ZnBr₂ catalysts

Catalyst	Run	X_G (%)	S_{GC} (%)	Y_{GC} (v)
PS-(Im) ₂ ZnBr ₂	1	65.8	72.3	47.6
	2	63.9	71.4	45.6
	3	60.8	70.7	43.0
	4	55.3	70.1	38.8
CS-(Im) ₂ ZnBr ₂	1	55.3	58.8	32.5
	2	45.8	56.9	26.1
	3	21.7	55.4	12.1
CH-(Im) ₂ ZnBr ₂	1	57.6	61.0	35.2
	2	57.2	47.1	26.9
	3	53.5	47.0	25.1
	4	52.5	46.5	24.4

Reaction conditions: Urea=50 mmol, Glycerol=50 mmol, Cat.=5 wt% of glycerol, Temp.=140 °C, Degree of vacuum=14.7 kPa, Reaction time=6 h

The relationships between the $\ln k_{app}$ values of different S-MIL catalysts and $1/T$ are shown in Fig. 9; these were subjected to linear regression. The activation energies were obtained by plotting $\ln k_{app}$ versus $1/T$, and the results are listed in Table 3, with the standard deviations. The order of the approximate activation energies is PS-(Im)₂ZnBr₂ (142.9 kJ)<CH-(Im)₂ZnBr₂ (163.0 kJ)<CS-(Im)₂ZnBr₂ (166.7 kJ); these results are consistent with the experimentally obtained activity order of the different S-MIL catalysts.

The stabilities of the catalysts were tested by reusing them four

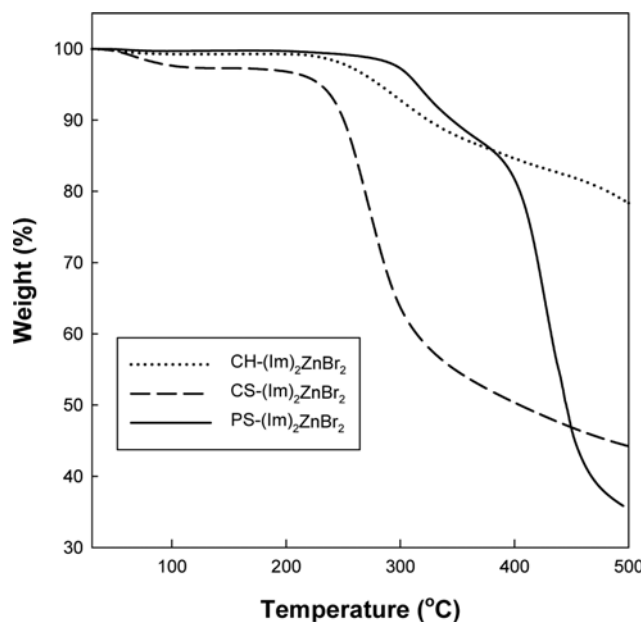


Fig. 10. Thermogravimetric analysis (TGA) of S-(Im)₂ZnBr₂ catalysts.

times, after separation from the reaction mixture at each experimental run, without reactivation (Table 4). The PS-(Im)₂ZnBr₂ and CH-(Im)₂ZnBr₂ catalysts maintained their activities, showing less than 20% loss of their initial activity after the fourth run. However, CS-(Im)₂ZnBr₂ could only be reused twice. This could be explained by the relatively low thermal stability of CS-(Im)₂ZnBr₂, as shown by TGA experiments (Fig. 10).

CONCLUSIONS

Three different S-MIL catalysts were synthesized and characterized by using various physicochemical methods. The S-MIL catalysts showed good catalytic activity for the synthesis of GC from urea and glycerol under mild reaction conditions. Detailed kinetic experiments and models for the reaction system over different S-MIL catalysts were developed, and a two-step reaction mechanism was proposed. The order of the approximate reaction rate constants for the immobilized catalysts was PS-(Im)₂ZnBr₂ > CH-(Im)₂ZnBr₂ > CS-(Im)₂ZnBr₂. The highest activity of PS-(Im)₂ZnBr₂ was considered to be due to its well-balanced acid-base properties. The catalyst can be reused with high possibility of easy recovery.

ACKNOWLEDGEMENTS

This study was supported by the Ministry of Education of Korea through National Research Foundation (2012-001507), Global Frontier Program, and KBSI.

REFERENCES

1. A. Behr, J. Enilting, K. Irawadi, J. Leschinski and F. Lindner, *Green Chem.*, **10**, 13 (2008).
2. A. S. Kovvali and K. K. Sirkar, *Ind. Eng. Chem. Res.*, **41**, 2287 (2002).
3. J. Rousseau and C. Rousseau, *Tetrahedron*, **65**, 8571 (2009).
4. M. Selva and M. Fabris, *Green Chem.*, **11**, 1161 (2009).
5. M. Ghandi, A. Mostashari, M. Karegar and M. J. Barzegar, *Am. Oil Chem. Soc.*, **84**, 681 (2007).
6. G. Rokicki, P. Rokoczy, P. Parzuchowski and M. Sobiecki, *Green Chem.*, **7**, 529 (2005).
7. Z. Mouloungui, J. W. Yoo, C. A. Gachen and A. Gaset, EP 0739888 (1996).
8. J. H. Teles, N. Rieber and W. Harder, US 5359094 (1994).
9. M. Aresta, A. Dibenedetto and C. Pastore, *Catal. Today*, **115**, 88 (2006).
10. Q. Li, W. Zhang, N. Zhao, W. Wei and Y. Sun, *Catal. Today*, **115**, 111 (2006).
11. M. Okutsu and T. Kitsuki, JP 039347 (2007).
12. M. Aresta, J. L. Dubois, A. Dibenedetto, F. Nocito and C. Ferragina, EP 08305653.1 (2008).
13. T. Sasa, M. Okutsu and M. Uno, JP 067689 (2009).
14. M. Okutsu and T. Kitsuki, JP 050415 (2000).
15. S. Fujita, Y. Yamanishi and M. Arai, *J. Catal.*, **297**, 137 (2013).
16. M. Aresta, A. Dibenedetto, F. Nocito and C. Ferragina, *J. Catal.*, **268**, 106 (2009).
17. C. Hammond, J. A. L. Sanchez, M. H. A. Rahim, N. Dimitratos, R. L. Jenkins, A. F. Carley, Q. He, C. J. Kiely, D. W. Knight and G. J. Hutchings, *Dalton Trans.*, **40**, 3927 (2011).
18. N. E. Leadbeater and M. Marco, *Chem. Rev.*, **102**, 3217 (2002).
19. C. A. McNamara, M. J. Dixon and M. Bradley, *Chem. Rev.*, **102**, 3275 (2002).
20. S. Bhattacharyya, *Comb. Chem. High Throughput Screen.*, **3**, 65 (2000).
21. T. Frenzel, W. Solodenko and A. Kirschning, in: R. Buchmeiser (Ed.), *Polymeric Materials in Organic Synthesis and Catalysis*, Wiley-VCH, Weinheim, 201-240 (2003).
22. Z. Guo, R. Xing, S. Liu, Z. Zhong and P. Li, *Carbohydr. Polym.*, **73**, 173 (2008).
23. C. T. Kresge, M. E. Leonowicz, W. J. Roth, J. C. Vartuli and J. S. Beck, *Nature*, **359**, 710 (1992).
24. H. L. Shim, S. Udayakumar, J. I. Yu, I. Kim and D. W. Park, *Catal. Today*, **148**, 350 (2009).
25. L. Han, H. Li, S. J. Choi, M. S. Park, S. M. Lee, Y. J. Kim and D. W. Park, *Appl. Catal. A Gen.*, **429**, 67 (2012).
26. D. W. Kim and D. W. Park, *J. Nanosci. Nanotechnol.*, **14**, 4632 (2014).
27. D. W. Kim, M. S. Park, G. A. Park, S. D. Lee, M. Selvaraj and D. W. Park, *Res. Chem. Intermed.*, **37**, 1305 (2011).
28. J. I. Yu, H. J. Choi, M. Selvaraj and D. W. Park, *React. Kinet. Mech. Catal.*, **102**, 353 (2011).
29. A. C. Kathalikkattil, J. Tharun, R. Roshan, H. G. Soek and D. W. Park, *Appl. Catal. A Gen.*, **447**, 107 (2012).
30. G. R. Krishnan and K. Sreeksumar, *Appl. Catal. A Gen.*, **353**, 80 (2009).
31. C. Qi, J. Ye, W. Zeng and H. Jiang, *Adv. Synth. Catal.*, **352**, 1925 (2010).
32. J. Sun, W. Cheng, W. Fan, Y. Wang, Z. Meng and S. Zhang, *Catal. Today*, **148**, 361 (2009).
33. J. Tharun, Y. S. Hwang, R. Roshan, S. H. Ahn, A. C. Kathalikkattil and D. W. Park, *Catal. Sci. Technol.*, **2**, 1674 (2012).
34. N. Vallapa, O. Wiarachai, N. Thongchul, J. Pan, V. Tangpasuthadol,

- S. Kiatkamjornwong and V. P. Hoven, *Carbohydr. Polym.*, **83**, 868 (2011).
35. I. Niedermaier, C. Kolbeck, N. Taccardi, P. S. Schulz, J. Li, T. Drewello, P. Wasserscheid, H. P. Steinruck and F. Maier, *Chem. Phys. Chem.*, **13**, 1725 (2012).
36. S. Abry, A. Thibon, B. Albela, P. Delichere, F. Banse and L. Bonneviot, *New J. Chem.*, **33**, 484 (2009).
37. D. Derouet, S. Forgeard, J. C. Brosse, J. Emery and J. Y. Buzare, *J. Polym. Sci. Pol. Chem.*, **36**, 437 (1998).
38. S. S. Silva, M. I. Santos, O. P. Coutinho, J. F. Mano and R. L. Reis, *J. Mater. Sci. Mater. Med.*, **16**, 575 (2005).
39. D. W. Kim, K. A. Park, M. J. Kim, D. H. Kang, J. G. Yang and D. W. Park, *Appl. Catal. A. Gen.*, **473**, 31 (2014).